Transitional forms in the *Eprolithus-Lithastrinus* lineage: a taxonomic revision of Turonian through Santonian species

Matthew J. Corbett and David K. Watkins
Department of Earth and Atmospheric Sciences, University of Nebraska-Lincoln, Lincoln, NE, 68588-0340, USA
email: mcorbett@unl.edu

ABSTRACT: The evolution of *Lithastrinus* from *Eprolithus* is observed in Turonian through Santonian material via variation in the number and morphology of wall elements. Previously, the shape of projections off the wall elements (rays) the size of the diaphragm, and inclination and twisting about the central area of the wall elements have been used to separate the genera, but these criteria are too general to consistently separate transitional 7-rayed forms. The more reliable criteria we have defined for distinguishing two different taxa, *Eprolithus moratus* and *Lithastrinus septenarius*, provides a more accurate biostratigraphic placement for these intermediate forms.

The younger late Turonian to middle Santonian form, *L. septenarius*, is separated from the older form, *E. moratus*, through reduced central depression size (<50% the width of the entire central area) and rays that are generally longer (>50% the width of the central area) and angled away from the ring of elements (>15°). In *Lithastrinus* the rays only project from the proximal and distal sides of the wall elements, while in *E. moratus* they extend as a single ridge between the two sides. When in the focal plane of the diaphragm the wall elements appear as a rounded collar in *L. septenarius*, which can also be used to differentiate between the two taxa, especially in poorly preserved material.

INTRODUCTION

Variation within the Polycyclolithaceae (Perch-Nielsen 1979; Varol 1992) has been long recognized and their use as important biostratigraphic markers is well documented (Stradner 1962; Forchheimer 1972; Thierstein 1973; Black 1973; Perch-Nielsen 1985; Varol 1992; Bralower and Bergen, 1998; Burnett 1998). Despite a relatively simple construction, a number of taxa have been clearly defined based on the variation in the shape, arrangement, and number of elements. One of the most biostratigraphically useful lineages in the Polycyclolithaceae is the mid-late Cretaceous evolutionary line from *Eprolithus floralis* (Stradner 1962) Stover 1966 to *Lithastrinus grilli*

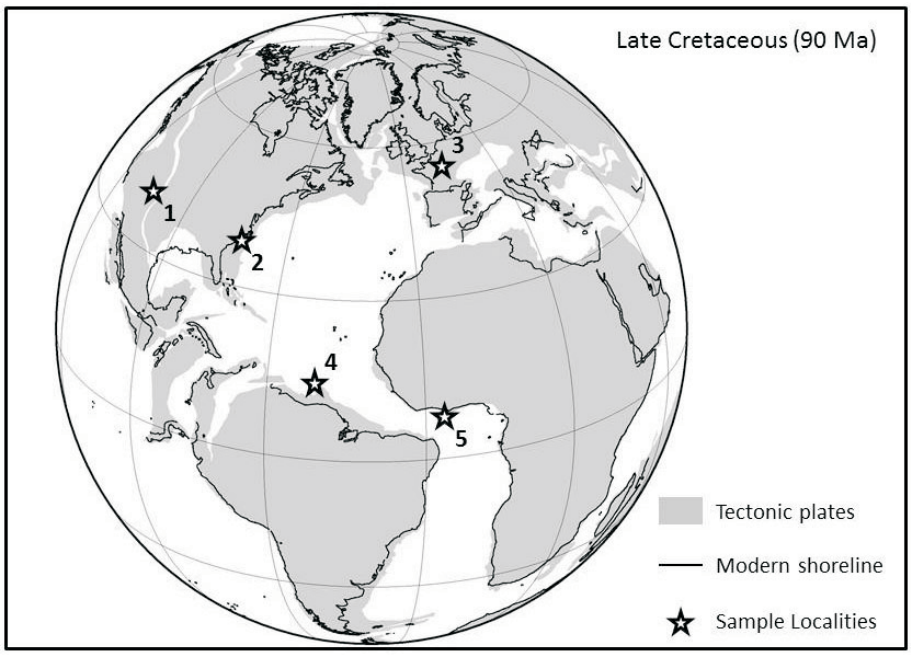

TEXT-FIGURE 1
Paleogeographic reconstruction of approximately 90 Ma showing the location of materials used in this study. Sites include: (1) the type section of the Mancos Shale at Mesa Verde National Park, CO; (2) USGS Kure Beach Corehole from Kure Beach, North Carolina; (3) material referred to in Stover (1966) from northern France; (4) Demerara Rise IODP Leg 207, Sites 1257B and 1259C; and (5) Côte D'Ivoire-Ghana Transform Margin Legs 159, Site 959D. (Created with the ODSN Plate Tectonic Reconstruction Service 2011).

Table 1
Samples and sites used in collecting photographs and/or morphological and biostratigraphic data in this study. Samples are assigned relative ages using the zonation of Sissingh (1977) as modified by Perch-Nielsen (1985) and qualitative descriptions of preservation.

Sample		Nannofossil Zone	Preservation
Kure Beach Corehole	NJ 1550 1090.3 ft	CC 16	excellent
	NJ 1551 1100.7 ft		excellent
	NJ 1554 1146.6 ft	CC 13	good-moderate
	NJ 1557 1165.4 ft		moderate
Leg 159	Site 959D, Core 66R, Section 6, 47-50 cm	CC 15	moderate-poor
	Site 959D, Core 66R, Section 7, 8-11 cm		moderate
	Site 959D, Core 67R, Section 2, 105-106 cm		good
	Site 960C, Core 26x, Section CC, top	CC 12	good
	Site 959D, Core 68R, Section 1, 14-15 cm	CC 11	moderate
Leg 207	Site 1257B, Core 19, Section 1W, 22-23 cm	CC 15	moderate-good
	Site 1257B, Core 19, Section 2W, 110-111 cm		moderate-poor
	Site 1259C, Core 11, Section 4W, 109-110 cm	CC 14	moderate-good
	Site 1259C, Core 11, Section 5W, 58.5-59.5 cm		good
	Site 1259C, Core 12, Section 1W, 12-13 cm		moderate
	Site 1259C, Core 12, Section 3W, 110-111 cm		moderate
	Site 1259C, Core 12, Section CCW, 11-12 cm	CC 13	good
	Site 1257B, Core 23, Section 1W, 10-11 cm	CC 11	good
Mesa Verde 44.4 m		CC 12	moderate-good
Stover 1966 Sample 9*		CC 12	very poor
Stover 1966 Sample 13		CC 11	poor

* Sample not used for morphological analysis

(Stradner 1962), which contributes several datums to global and regional zonal schemes (e.g., Perch-Nielsen 1985; Varol 1992; Burnett 1998; Bralower and Bergen 1998). Confusion remains regarding the identification of transitional forms between these two genera and past taxonomic revisions have caused disagreements about the identification of species and their true first occurrences (Stover 1966; Forchheimer 1972; Varol 1992).

A number of transitional forms between the end members *E. floralis* (9 rays) and *L. grillii* (6 rays) have been described and differences between the 7-rayed taxa (*L. septenarius, E. moratus*, and *E. eptapetalus*) are not clearly understood. These taxa record a key evolutionary change in the Polycyclolithaceae during the Turonian and Coniacian, from the petal-like elements and large diaphragm of *Eprolithus* to the longer, pointed and twisted rays along with a reduced diaphragm of *Lithastrinus*.

Review of the type descriptions and new observations detailed in this study illustrate inadequacies in the current definitions of *Eprolithus eptapetalus* (Varol 1992) and *Lithastrinus moratus* (Stover 1966) Varol 1992 and the status of original type material described by Stover (1966) and Forchheimer (1972). This study presents both a quantitative and qualitative criteria consistent for distinguishing both intermediate forms between *Eprolithus* and *Lithastrinus*.

MATERIALS AND METHODS

Five sites were chosen to analyze the full stratigraphic range of intermediate 7-rayed forms. These sites are detailed in Figure 1 and a summary of the materials used is presented in Table 1. A total of 428 specimens were observed in Turonian, Coniacian, and Santonian material from ODP Legs 159 Site 959D (Côte D'Ivoire-Ghana Transform Margin, Equatorial Atlantic), Leg 207 Sites 1257B and 1259C (Demerara Rise, Western Atlantic), the USGS Kure Beach Corehole NH-C-1-2001 (Kure Beach, North Carolina), and from outcroppings at Mesa Verde National Park, Colorado (Western Interior Seaway). Lithostratigraphic, biostratigraphic, and sedimentologic information for the Kure Beach Corehole was provided by J. Self-Trail (pers. comm., 2012). The lithostratigraphy and sedimentology of the Mesa Verde section is described in Leckie et al. (1997) and corresponding foraminiferal assemblage data is presented in West et al. (1998) and Leckie et al. (1998) Topotype specimens of *Lithastrinus moratus* (Stover 1966) from France were also examined. Slides were prepared using the double slurry and settling methods detailed by Watkins and Bergen (2003) and Geisen et al. (1999), respectively.

Calcareous nannofossils were studied using a Zeiss Photoscope III at a total magnification of ×1250 using cross-polarized light, plane light, phase contrast, and through a one-quarter mica plate. Morphological data were collected from digital photomicrographs with photo processing program ImageJ (Rasband, 1997–2012). Additional specimens were examined using a Hitachi S-3000N variable pressure and a S4700 field emission scanning electron microscope (SEM).

Four measurements, labeled in text-figure 2, were taken for each specimen examined. The diameter of the central area and that of the central depression were collected because the size of the diaphragm which forms the base of the depression is used as a distinguishing characteristic by other workers separating *Lithastrinus* from *Eprolithus* (Varol 1992; Bralower and Bergen 1998). The length of the rays and the ray angle was also measured. Ratios comparing the size of the central depression ver-

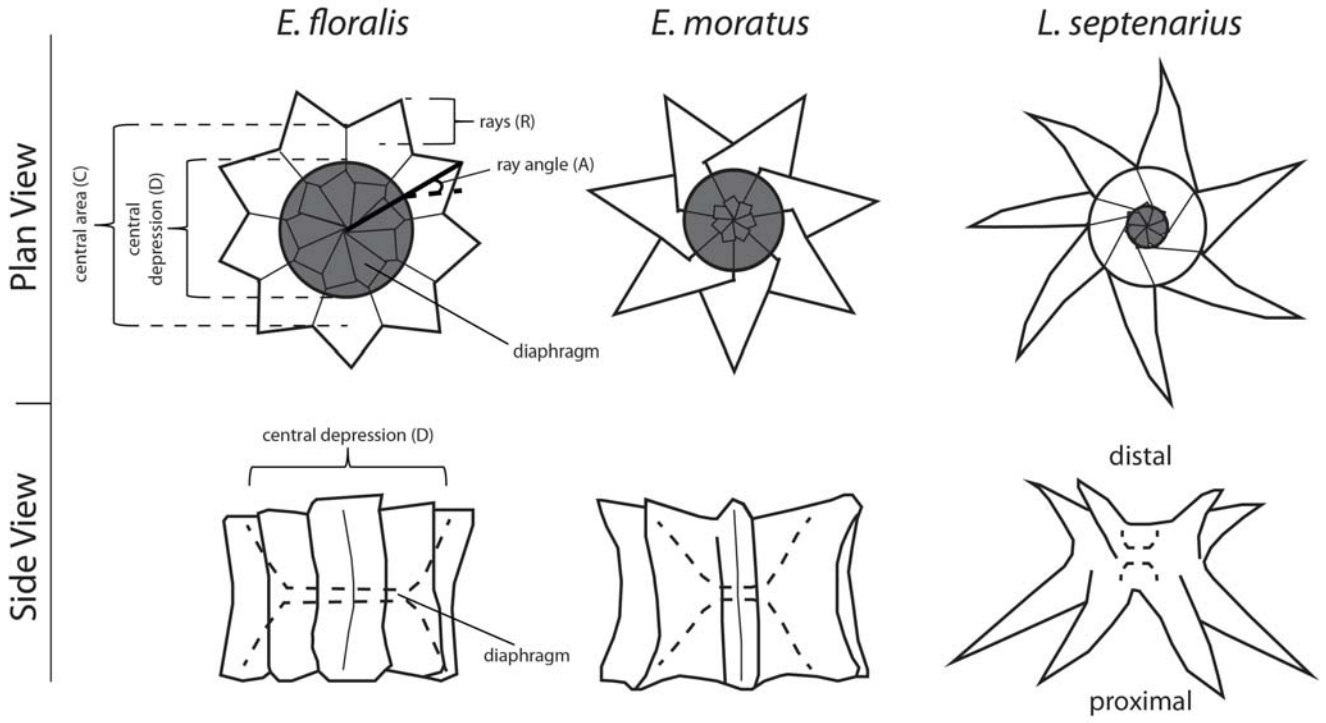

TEXT-FIGURE 2
Illustration showing basic morphology of *Eprolithus* and *Lithastrinus* in plan and side view. *Eprolithus floralis*, the type species of *Eprolithus*, is shown with labels indicating measurements taken in this study from intermediate taxa *Eprolithus moratus* and *Lithastrinus septenarius*. These measurements are: width of the central area from the outside edge of the elements between rays (C), width of the central depression (D), length of the rays (R), and ray angle (A). The grey shaded areas represent regions typically dark or dull in polarized light and correspond to the area of the thinner central depression. Dashed lines show internal structure visible when focusing in side view. Note that the diaphragm that connects the wall elements is actually smaller in *E. moratus* than in *E. floralis,* while the central depression remains relatively large, compared to *Lithastrinus*.

sus the central area (D/C) and length of the rays versus the central area (R/C) were used as measures of size variations, which ranged widely throughout the studied successions. These data were analyzed using the paleontological statistics program PAST (Hammer and Harper 2006).

CURRENT AND HISTORICAL TAXONOMY

Eprolithus and *Lithastrinus* are similar in that they have a central area surrounded by a wall of elements arranged in two cycles around a central depression connected by a thin layer of flat overlapping elements, called the diaphragm (text-fig. 2). Rays are an extension of each of the wall elements that project away from the central area. Stradner's (1962) original description of the genus *Lithastrinus* included many different forms later separated into the genus *Eprolithus* by Stover (1966). Stover argued that *Eprolithus* have a more circular to "sun-shaped" outline and an "H" shape in cross-section where the large diaphragm connects between the cycles (text-fig. 2; Pl. 1, fig. 6; Pl. 2, fig. 5), differing from *Lithastrinus* which have a less conspicuous opening and longer attenuated rays (text-fig. 2; Pl. 1, fig. 5; Pl. 2, fig. 6). In his extensive revision of the Polycyclolithaceae, Varol (1992) added that the elements in both genera may be slightly inclined around the central area, though in *Lithastrinus* they are strongly inclined and twisted. The type species for *Eprolithus* and *Lithastrinus*, (*E. floralis* and *L. grillii)*, are shown in text-igure 6 and Plate 2 for comparison to their 7-rayed transitional forms.

The number of elements/rays in *Eprolithus* decreases from the 9 *(E. floralis)* to 8 *(Eprolithus octopetalus)* (Varol 1992) at the Cenomanian–Turonian boundary (see Varol 1992, Pl. 1, Figs. 5–10; Pl. 6, Figs. 14–15; this paper, Pl. 1, figs. 3–4; Pl. 2, fig. 4). At roughly the same stratigraphic level Stover (1966) describes the appearance of a form that continues through the Turonian with as few as 7 elements which he placed in the genus *Lithastrinus* as *L. moratus* (see Stover 1966, Pl. 7, Fig. 20; this paper, text-fig. 2). He describes *L. moratus* as having overlapping twisted segments that are lanceolate in plan view contrasting with *L. grilli* (Pl. 1, fig. 4; Pl. 2, fig. 6) which has fewer, more attenuated elements. A second 7-rayed form, *Lithastrinus septenarius* (Forchheimer 1972), was described with long triangular rays more closely resembling *L. grilli* (see Forchheimer 1972, Pl. 24, Figs. 1–4; Pl. 27, Fig. 2).

Unfortunately the type material in Forchheimer (1972) was incorrectly correlated to macrofossil biostratigraphy, and thus the type levels of most of the new species presented therein are offset by several stages. *Lithastrinus septenarius* occurs with *Marthasterites* and *Micula* taxa through the entirety of the borehole material examined (see Forchheimer 1972, Figs. 11–12). *Marthasterites* taxa first appear in the upper Turonian and are generally more common in the Coniacian, while species of *Micula* first occur in the lower-middle Coniacian. This suggests at least a Coniacian age for the *L. septenarius* topotype material.

Varol (1992) revised the taxonomic definitions of *L. moratus* and *L. septenarius* and described a new 7-rayed taxa, *Eprolithus*

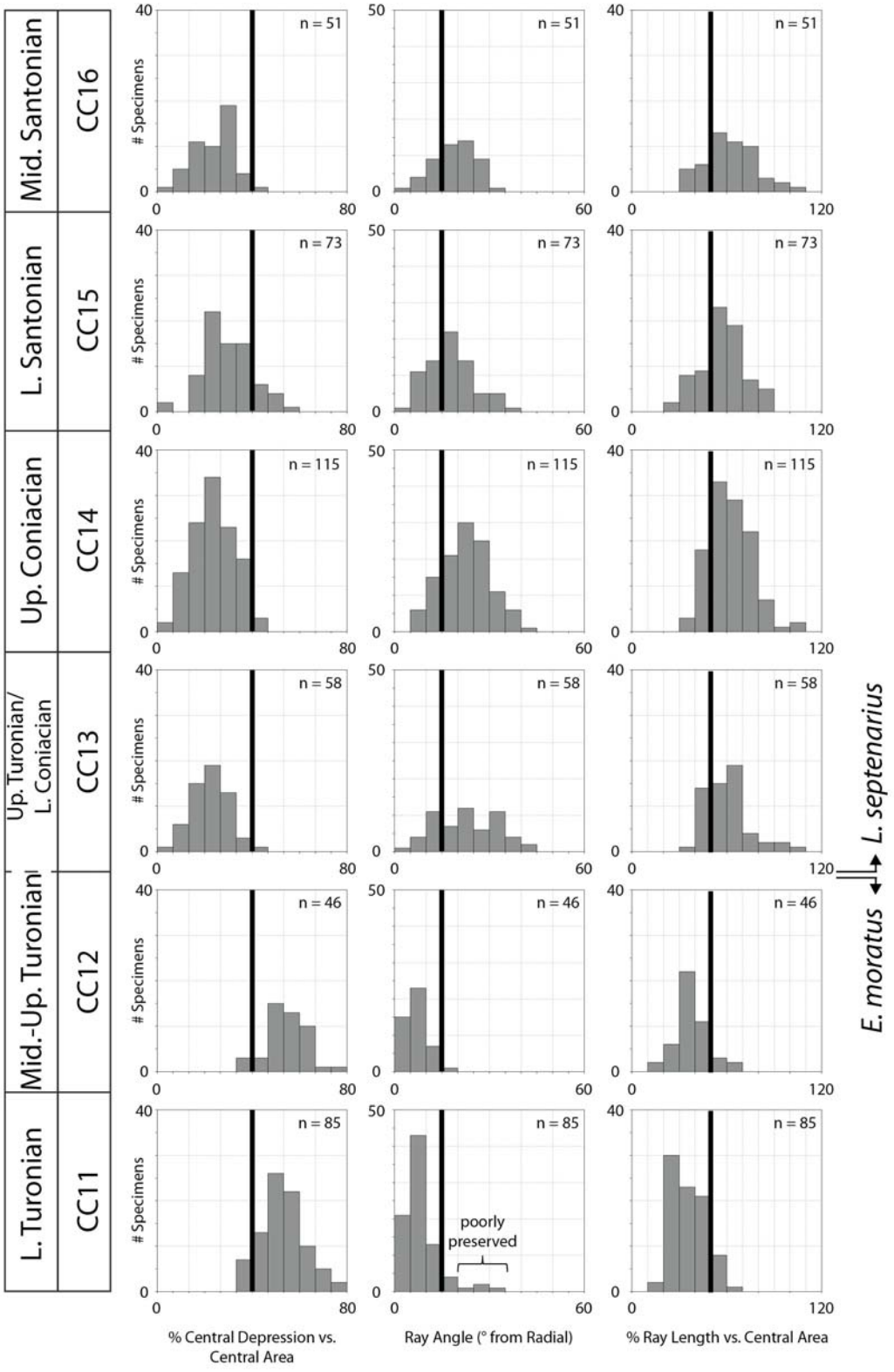

TEXT-FIGURE 3
A series of histograms arranged according to the Sissingh (1977) nannofossil zonation showing morphometric data collected from 7-rayed specimens in this study. The average angle of the rays from radial orientation (or straight from the center of the specimen) and relative size of the central depression vs. central area and ray length vs. central area width are shown. Vertical thick black line indicates proposed cutoff criteria for differentiating between the two transitional species E. moratus and L. septenarius, the interpreted ranges of which are shown at right. Note the poorly preserved specimens in CC11, which were measured from the type material for E. moratus (Stover 1966). These serve to highlight the caution which must be used when seprating these taxa in overgrown samples.

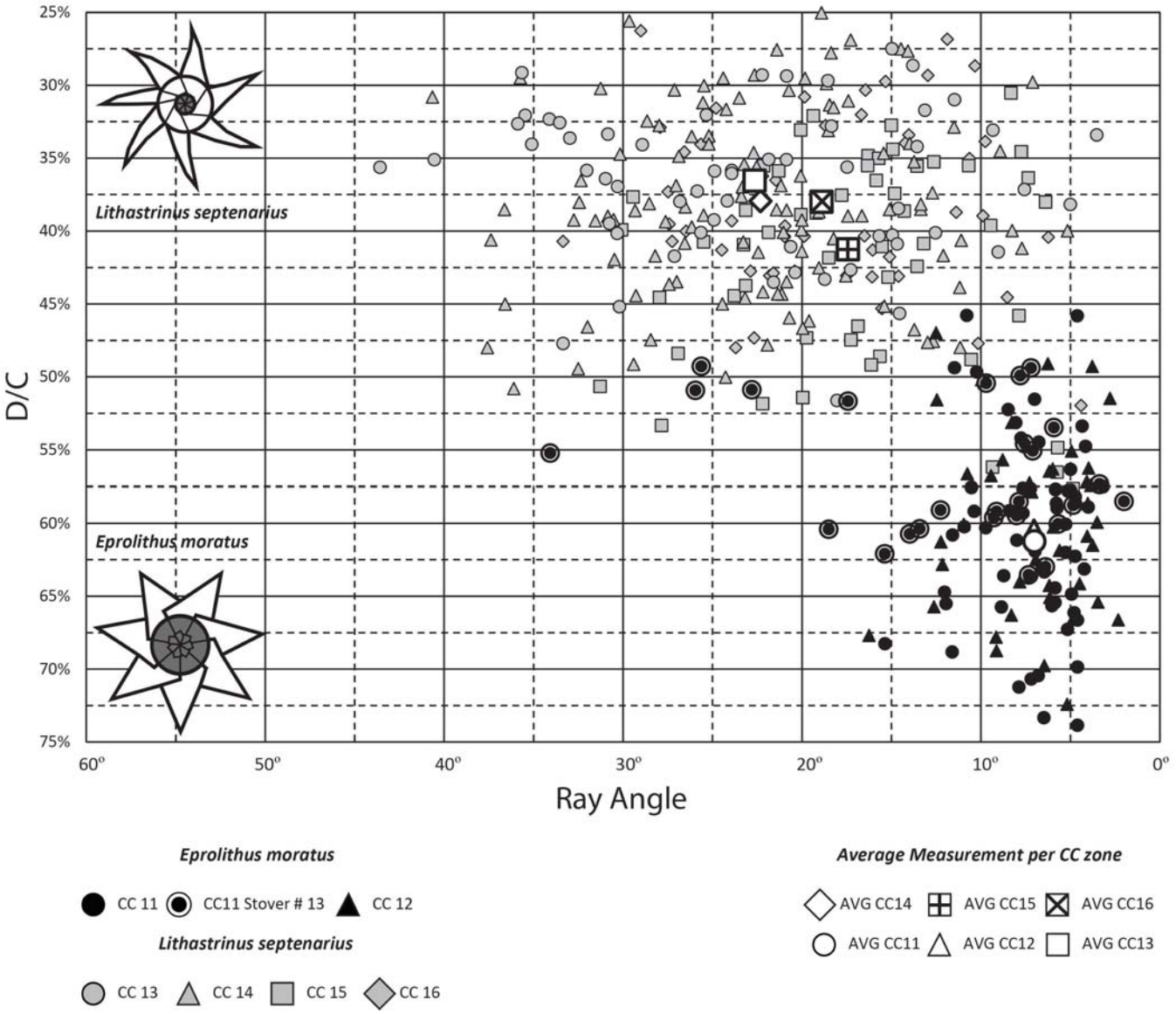

TEXT-FIGURE 4
XY scatterplot of important measurements and/or ratios used for differentiating transitional species. The average angle of the rays from radial (Ray Angle) and relative size of the central depression vs. central area (D/C) are plotted. *E. moratus* (CC11-12) is highlighted in black points with measurements of specimens from the Stover (1966) topotype material shown with white borders and *L. septenarius* (CC13-16) in grey. Averages for each CC zone are also plotted in white. Note how the two taxa are separated into two distinct groups using these measurements.

eptapetalus. *Lithastrinus septenarius* was given junior synonym status under *L. moratus*, arguing that Stover's (1966) type specimens are overgrown highly twisted forms. *Eprolithus eptapetalus* is described as having 7 petal-like elements that may be short and rounded or long and pointed that ranges from lower Turonian through lowermost Coniacian (see Varol 1992 Pl. 1, Figs. 2–4; Pl. 6, Figs. 8–13).

RESULTS

Observations of 7-rayed Eprolithus and Lithastrinus forms from the Turonian through Santonian suggest the morphology of the lineage changes abruptly in the upper Turonian. The size of the central depression/diaphragm decreases, angle of the rays increases, and the relative length of the rays increases between nannofossil zones CC12 and CC13 of Sissingh (1977) and Perch-Nielsen (1985). This is demonstrated by plotting depression/diaphragm diameter and ray angle measurements against age for each nannofossil zone as a series of histograms and as a scatter plot (text-figs. 3–4). Representative photomicrographs from light microscopy and SEM of the 7-rayed intermediate forms are presented in Plates 1–6.

The oldest specimens from the lower to middle Turonian exhibit a morphotype with relatively short, petal-like elements and a wide central depression that is easily distinguished in moderate to well preserved material in the light microscope from younger *Lithastrinus* species (e.g., text-fig. 3; Pl. 3, figs. 1–2; Pl. 4, figs.

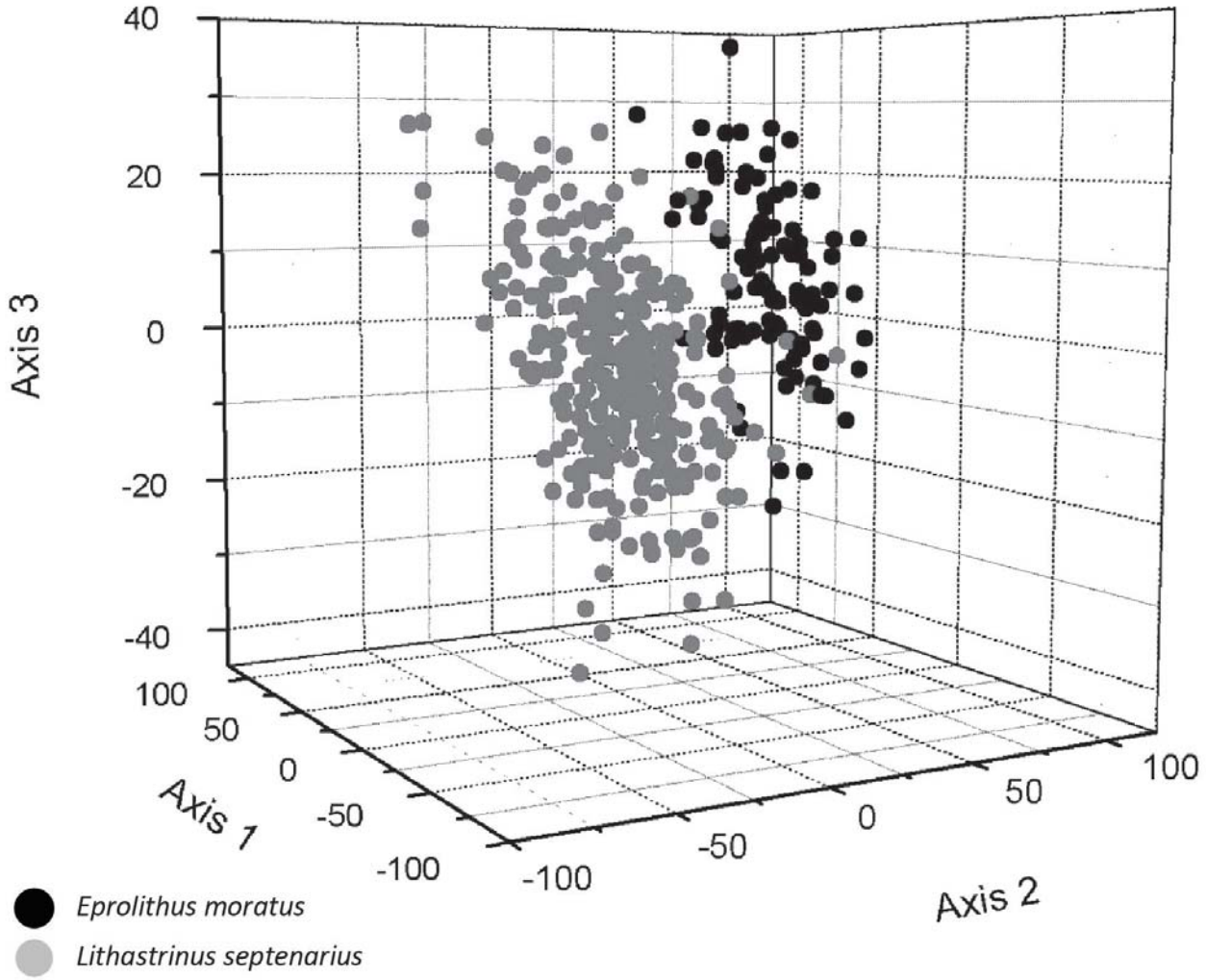

TEXT-FIGURE 5
XYZ Plot of PCA axis values for specimens. *E. moratus* (CC11-12) is highlighted in black points and *L. septenarius* (CC13-16) in grey. Note how the two taxa separate into two distinct groups, particularly PCA Axis 2, which has a high loading with respect to size of the central depression (0.68).

1–6). These elements can appear thick and rounded (Pl. 3, fig. 3; Pl. 6, figs. 1–2) or more pointed and petal-like (Pl. 4, fig. 1–2, 4; Pl. 6, figs. 3–4). This superficial difference in appearance is not reflected in biometric data and is in fact a variation found within *E. floralis* and *E. octopetalus* (e.g. Pl. 1, figs. 1–4). The length of the rays in proportion to the width of the central area (L/C) plot as one population which averages 36.8 % for 7-rayed specimens from nannofossil zones CC11 and CC12 (text-fig. 3).

The central depression of the earliest 7-rayed forms from the lower Turonian have a diameter comprising ~50–75% of the width of the entire central area (D/C) with an average value of 60% (text-fig. 3, 4). This wide, thin area is relatively dull compared to the thick outer wall elements and is first order grey to a pale yellow in well preserved specimens (e.g., Pl. 3, figs. 1–2). SEM photomicrographs reveal that the diaphragm of overlapping plates is already reduced in size in this 7-rayed morphotype (Pl. 3, figs. 1, 4) compared to that of the 9-rayed *E. floralis* (Pl. 2, figs. 1–2) and may have decreased in size through the evolution of *E. octopetalus* (Pl. 2, fig. 4). The central depression remains a wide feature and it is the inward growth of the wall elements that creates the appearance of a brighter central area and smaller diaphragm in *Lithastrinus* (Pl. 1, fig, 5b; Pl. 2, fig. 6).

At the extreme proximal and distal ends of the wall/ray elements *Eprolithus* specimens can appear slightly twisted. Focusing through *Eprolithus* forms, including the 7-rayed morphotype, shows that the rays are in focus and maintain a relatively constant angle (5–15°) and length between the proximal and distal sides (Pl. 3, figs. 1–2). SEM photomicrographs in Plate 2, figures 3 and 5 and Plate 4, figure 5 show this feature clearly, particularly Pl. 2, fig. 5, which shows an *E. floralis* specimen which has lost several elements on one wall cycle revealing the shape of the rays where they cross the diaphragm. This is consistent with Stover's (1966) description of *Eprolithus* as having an "H"-shaped side profile (Pl. 1, figs. 6–7).

The upper Turonian through Santonian specimens have a relatively smaller central depression and typically longer rays than *Eprolithus* species (text-figs. 3–4), generally fitting within the definition of *L. moratus* as suggested by Varol (1992). The aver-

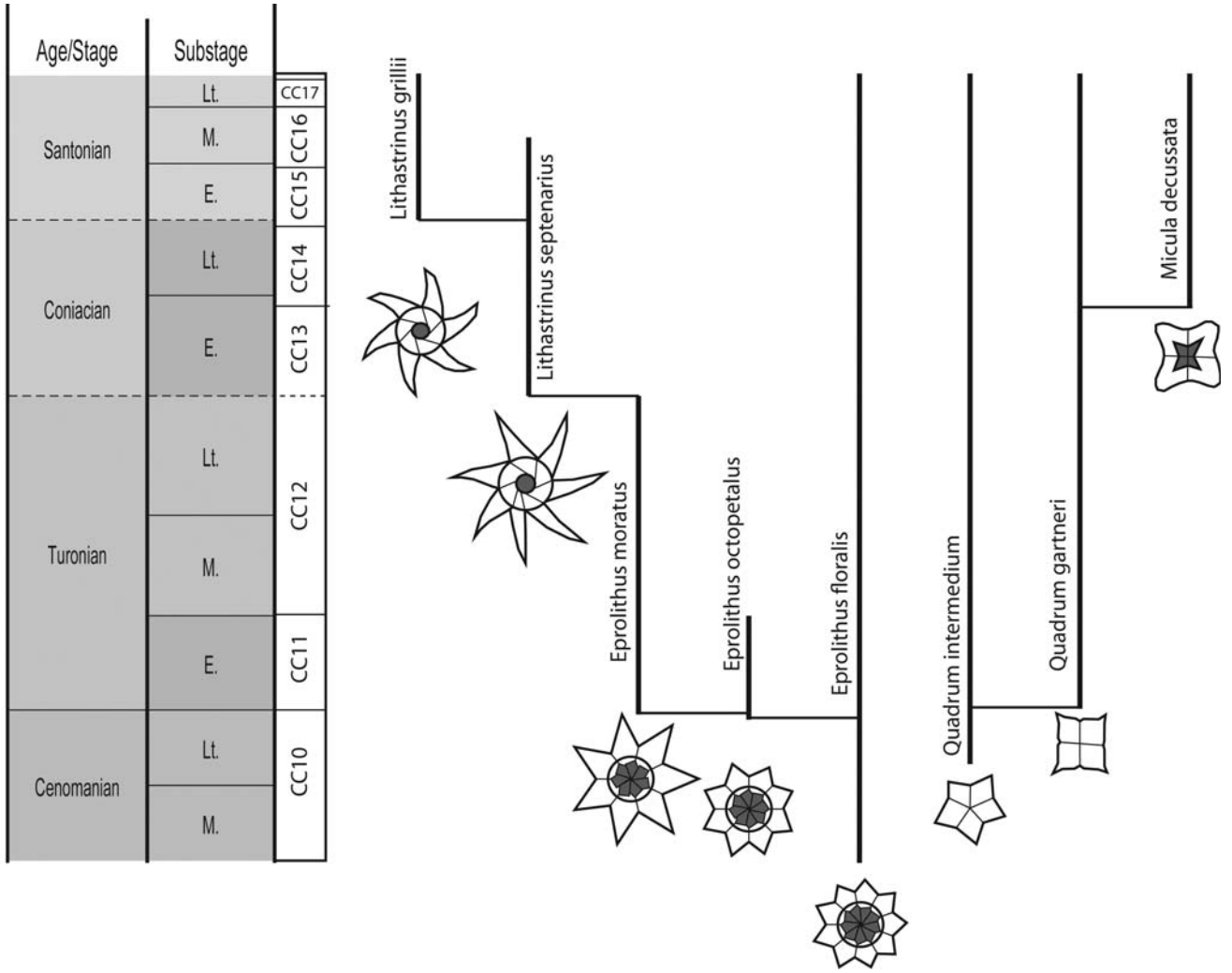

TEXT-FIGURE 6
Biostratigraphic range chart for the evolutionary lineage between *Eprolithus floralis* and *Lithastrinus grillii* as well as other important Polycyclolithacean markers. Time scale and CC nannofossil zonations (Perch-Nielsen 1985) modified from Gradstein et al. 2004. Nannofossil ranges based on results from this study and Varol (1992). (Timescale produced with TS Creator, Ogg and Lugowski 2004).

age D/C value decreases to ~37% in the upper Turonian and remains consistent, ranging between 25–50%, through the lower-middle Santonian (CC16). This form is clearly distinct from lower-middle Turonian specimens, as is indicated in Figure 4. In the light microscope, the central area is bright since the outer wall elements are thicker and spin slightly when focusing as an expression of the increased twisting of these elements around the diaphragm (Pl. 3, fig. 3–4). The rays can be longer and either straight or slightly curved along their length, though this difference seems to be largely an effect of preservation (i.e., poor vs. good). In well preserved specimens it is also apparent that the rays are consistently longer on one side (designated here as the proximal side for consistency) of the fossil, as can be seen while focusing through specimens in plan view (Pl. 3, figs. 3–4; Pl. 5, figs. 1–4) and in side view (e.g. Pl. 1, fig. 8; Pl. 5, figs. 5–6).

The wall elements of *Lithastrinus* in the focal plane of the diaphragm form a nearly perfect round outline (e.g. Pl. 1, figs. 5b–d; Pl. 3, figs. 3d, 4d). This is frequently observed in poorly preserved material where the rays break off. The rays only protrude from the proximal and distal ends of *Lithastrinus*, unlike in *Eprolithus* where the rays form a continuous ridge between the two cycles. The rays taper inward towards the connection between the proximal and distal cycles as is evident from Pl. 2, fig. 6 of a *L. grillii* which has lost one cycle of wall elements. The rays also do not line up perfectly since the wall elements are more strongly twisted with an average angle from radial of 21° and ranges from ~4–44°. Despite this wide range in ray angle there is no indication that a separate species of 7–rayed *Lithastrinus* should be differentiated. This variation between CC13 and CC16 can most likely be explained by the combination of measurements from proximal and distal sides of specimens.

Principle Components Analysis (PCA) of the four measurements taken (text-fig. 5), excluding the poorly preserved Stover (1966) type material, shows the variance across the dataset to be nearly split between axes PCA1 and PCA2 (~48% and ~40% respectively). Loadings on PCA1 are dominated by overall central

area diameter (0.72) and ray length (0.66), reflecting the overall increase in size through time of *Eprolithus* to *Lithastrinus*. PCA2 is affected primarily by the size of the central depression (0.68) and is negatively correlated to ray length (-0.59). This is consistent with the use of the central depression or diaphragm size to separate the genus *Eprolithus* from *Lithastrinus*. The two taxa, as defined here, are clearly separated in diagrams plotting PCA and morphological values (text-figs. 3–5).

Many of the measurements taken could be influenced by preservation, as rays and diaphragms can dissolve or overgrow. Careful comparison between well preserved and poorly preserved specimens reveals the key features that can allow for consistent separation of the two 7-rayed morphotypes. In overgrown specimens the twisted proximal and distal ends of the ray elements overgrow and can superficially make any *Eprolithus* species appear similar to *Lithastrinus*. The central depression may also be artificially decreased in width by inward overgrowth of the wall elements (e.g. Pl. 4, fig. 6). By careful focusing through the specimens it is possible to determine whether the rays protrude completely between the proximal and distal sides or form a smoother rounded wall around the diaphragm with protrusions restricted to the proximal and distal ends of the wall elements. These observations are supported by SEM images (e.g. Pl. 4, fig. 5).

Examination of Stover's (1966) type material reveals that the 7-rayed morphotype he described is, in fact, an *Eprolithus* equivalent to that described as *E. eptapetalus* by Varol (1992). Despite very poor preservation it is clear that the specimens belong to *Eprolithus* and have rays which protrude along the length of the wall elements (Pl. 6, figs. 5–6). These poorly preserved specimens are presented in the charts and diagrams (e.g. text-fig. 4) to illustrate the appearance of twisted *Lithastrinus*-like rays in overgrown *Eprolithus*.

Conversely, Forchheimer's (1972) SEM photomicrographs of *L. septenarius* show a morphotype with long rays connected by a small, round ring of wall elements that is consistent with the uppermost Turonian through Santonian *Lithastrinus* morphotype described in this study. Since Stover and Forchheimer's type specimens are clearly distinct from one another they should be considered to be valid, and therefore *E. moratus* has priority over *E. eptapetalus,* rendering it invalid. SEM and light microscope photomicrographs taken at three different focal planes through specimens of different age and preservation support this conclusion (Pl. 3, figs. 3a–4e; Pl. 6, figs. 5a–6d).

BIOSTRATIGRAPHY

These species, like many others within the Polycyclolithaceae, are zonal markers because of their robust dissolution resistant construction and largely cosmopolitan distribution. The biostratigraphic ranges of the *E. floralis* through *L. grillii* lineage are illustrated in Figure 6 and plotted against the CC nannofossil zonation scheme as calibrated by Gradstein et al. (2004).

The ranges of *E. moratus* and *L. septenarius* are inconsistent with their placement in widely used biostratigraphic zonation schemes. *Marthasterites furcatus* (Deflandre in Deflandre and Fert 1954) Deflandre 1959 and *Liliasterites* spp. Stradner and Steinmetz 1984 are used to identify the upper Turonian in the CC and UC nannofossil zonations, but are often diachronous and unreliable in higher latitudes (Perch-Nielsen 1985; Watkins et al. 1998; Lees 2002). Additionally, the ranges of *Eiffellithus eximius* (Stover 1966) Perch-Nielsen 1968 and *M. furcatus* vary greatly between the two zonation schemes; both taxa are reported in either the lower or upper Turonian depending on the scheme (Perch-Nielsen 1985; Lees 2002; Lees 2008; Shamrock and Watkins 2009). Although *E. moratus* should co-occur with these taxa they were not observed together in this study. The First Occurrence (FO) of *L. septenarius* occurs earlier than predicted at Demerara Rise before the FO of *M. furcatus* and *Liliasterites* spp. and this species does not go extinct until after the FO of *Lucianorhabdus cayeuxii* Deflandre 1959 in the Kure Beach Core. This range is consistent with more recent zonation schemes (basal UC9 to base of UC12 in Lees 2002; 2008).

PLATE 1

Light photomicrographs of select Polycyclolithaceae at ×1250 magnification. Scale bar at bottom right is 10 micrometers. XPL = cross polarized light, PL = plane light, PC = phase contrast.

1 *E. floralis*, m. Cenomanian, Mesa Verde, 44.4 m; 1a: XPL, 1b: PC.

2 *E. floralis*, e. Turonian, Site 959D, Core 68R, Section 1, 14–15cm; 2a: XPL, 2b: PC.

3 *E. octopetalus*, e. Turonian, Site 959D, Core 68R, Section 1, 14–15cm; 3a: XPL, 3b: PL.

4 *E. octopetalus*, e. Turonian, Site 959D, Core 68R, Section 1, 14–15cm; 4a: XPL, 4b: PC.

5 *L. grillii*, m. Santonian, Kure Beach Corehole, 1100.7 ft; 5a: high focus on rays, XPL, 5b: low focus on diaphragm and "collar" of wall elements, XPL, 5c: high focus on rays, PC, 5d: low focus on diaphragm and "collar" of wall elements, PC.

6 *E. floralis* in side view, e. Turonian, Site 959D, Core 68R, Section 1, 14–15cm; XPL.

7 *E. moratus* in side view, e. Turonian, Site 959D, Core 68R, Section 1, 14–15cm; XPL.

8 *L. septenarius* in side view, Site 1259C, Core 12, Section 1W, 12–13cm; 8a: XPL, 8b: PC.

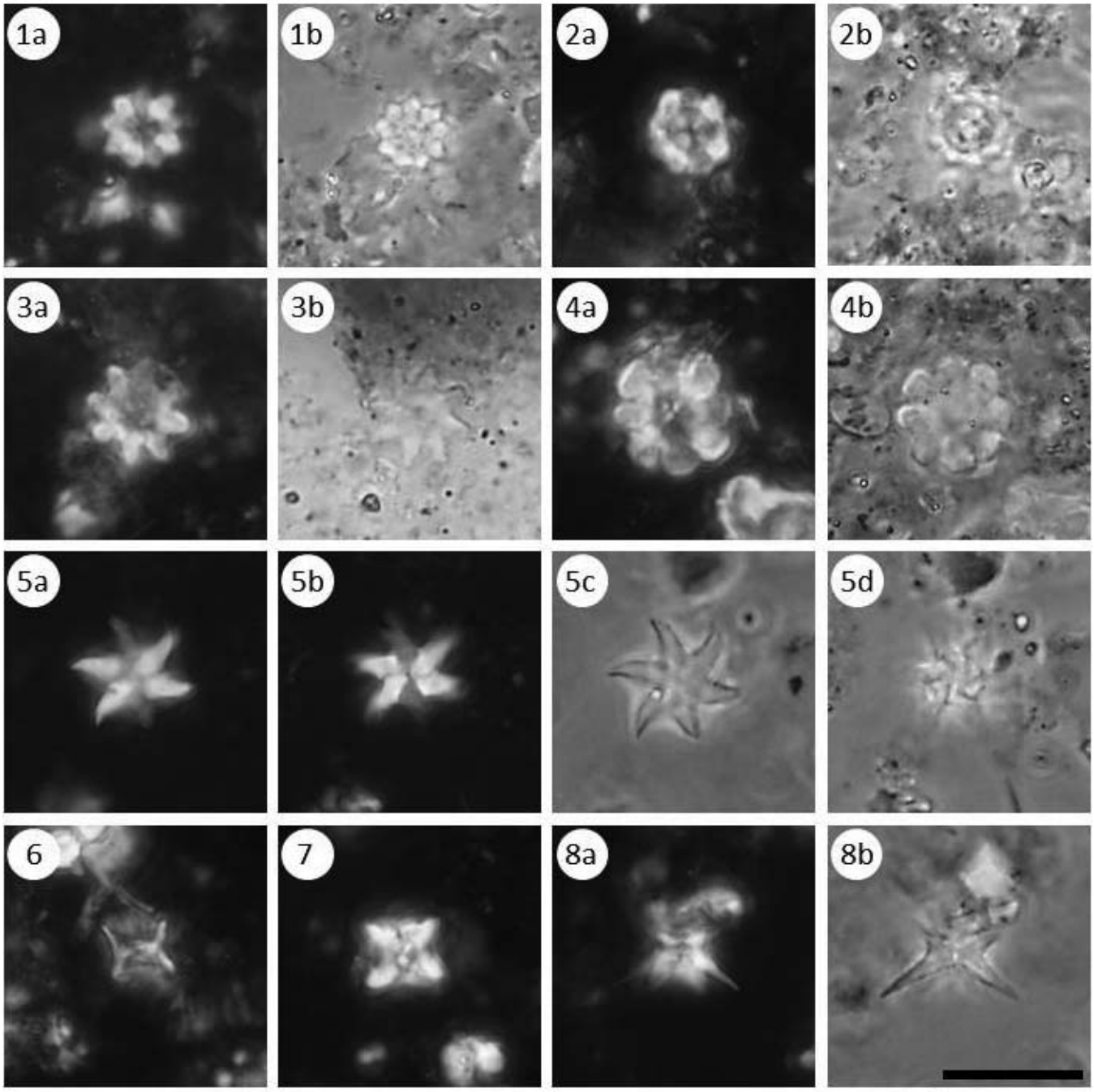
1a
1b
2a
2b
3a
3b
4a
4b
5a
5b
5c
5d
6
7
8a
8b

Eprolithus moratus first occurs as very rare specimens in the uppermost Cenomanian, close to the FOs of *E. octopetalus* and *Quadrum gartneri* Prins and Perch-Nielsen in Manivit et al. 1977 (Watkins 1985; Bralower and Bergen 1998; Hardas and Mutterlose 2006; Linnert et al. 2010). While there are possibly two different morphotypes based on superficial differences in ray shape, there is no recorded difference in stratigraphic range and they generally co-occur. This may be the source of some confusion in taxonomy and they are lumped together here. *Eprolithus moratus* is most abundant in the lower-mid Turonian, becoming very rare in the upper Turonian. It is not present above this level in the material examined in this paper (text-figs. 3–4), nor does it co-occur with *E. eximius* or *M. furcatus*. A few rare occurrences have been observed in Coniacian sections of other studies (e.g. Watkins et al. 1998), though it is likely an issue with species concepts or reworking.

The FO of *L. septenarius* had been used as the base of calcareous nannofossil zone CC13b, and is placed between the FOs of *M. furcatus* and *Micula decussata* Vekshina 1959 in the amended Sissingh (1977) zonation of Perch-Nielsen (1985). Its last occurrence (LO) was used as a secondary marker for the base of CC16. Using the morphological criteria proposed in this paper the FO of *L. septenarius* would appear to be in the uppermost Turonian or basal Coniacian. The last occurrence is above that of the FO of *L. cayeuxii* in the lower Santonian.

E. moratus and *L. septenarius* do not co-occur in any of the samples examined in this study. Specimens from CC15 that plot with older specimens of *E. moratus* (see text-fig. 4) have rays that project only from the proximal and distal ends of each wall element, suggesting they are actually *Lithastrinus*. The rapid transition between the two taxa in the uppermost Turonian and the stable morphology of the populations below and above this event may reflect a punctuated evolution between *Eprolithus* and *Lithastrinus*, a pattern not uncommon among the Polycyclolithaceae. Many sections across the Turonian-Coniacian boundary are separated by an unconformity which might explain the lack of any transitional overlap record.

SYSTEMATIC PALEONTOLOGY

FAMILY Polycyclolithaceae (Forchheimer 1972) Varol 1992
GENUS Eprolithus (Stover 1966) Varol 1992
Type species: *Lithastrinus floralis* Stradner, 1962

Eprolithus moratus (Stover) Burnett
Plate 1, figure 7; Plate 3, figures 1–2; Plate 4, figures 1–6; Plate 6, figures 1–6.

Eprolithus moratus (Stover 1966) Burnett in BOWN 1998
Eprolithus eptapetalus VAROL 1992 Pl. 1, Fig. 2–4; Pl. 6, Fig. 8–13
Lithastrinus moratus STOVER 1966 Pl. 7, Fig. 20

Diagnosis: An *Eprolithus* consisting of 7 wall elements surrounding a wide central depression no less than half the width of the central area, connected by a small diaphragm. Rays project as a ridge in a radial fashion from the wall elements to typically no more than a 15° angle.

Description: Seven wall elements are arranged vertically in a ring of two stacked cycles around a central depression. These cycles are connected in the middle of this central depression by

---

PLATE 2

SEM Photomicrographs of select Polycyclolithaceae species. Scale bars are 1 micrometer.

1 *E. floralis*, e. Turonian, Site 1257B, Core 23, Section 1W, 10–11cm; ×10,000.

2 Detail of specimen in 1 showing construction of the diaphragm; ×25,000.

3 *E. floralis* missing portions of one cycle of wall elements revealing shape of rays at intersection with the diaphragm, e. Turonian, Site 1257B, Core 23, Section 1W, 10–11cm; ×15,000.

4 *E. octopetalus*, e. Turonian, Site 1257B, Core 23, Section 1W, 10–11cm; ×10,000.

5 *E. floralis* oblique view showing shape of rays in profile, e. Turonian, Site 1257B, Core 23, Section 1W, 10–11cm; ×10,000.

6 *L. grillii* with one cycle missing showing the rounded, "collar"-like shape of the wall elements around the diaphragm, m. Santonian, Kure Beach Corehole, 1100.7 ft; ×15,000.

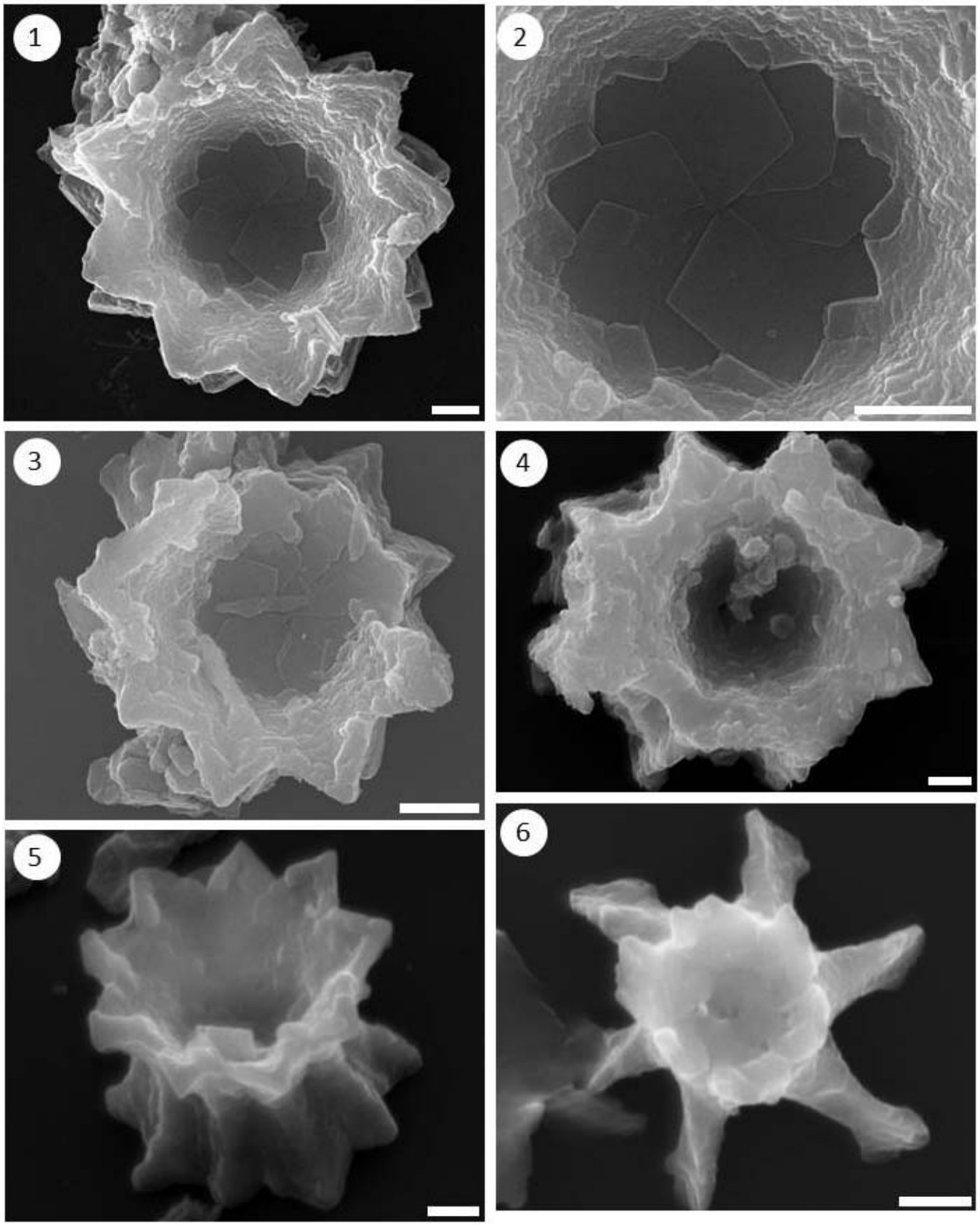
1
2
3
4
5
6

a thin plate, or diaphragm, of 7 overlapping lath-shaped elements. The central depression is wide and greater than half the width of the central area measured across the wall elements between the rays. The central depression appears dull in polarized light, giving the impression of a thin, wide diaphragm; however, in SEM the diaphragm is much smaller than the central depression itself (Pl. 4). Rounded to pointed rays project radially from the wall elements in a rosette or petaloid pattern and form a continuous ridge between the two cycles. A slight twisting of these rays may be evident at the proximal or distal end of each element, but generally they remain at less than 15° angle.

Measurements:

Central area width: 2.6–6.4µm, avg. = 3.9µm, n = 105

Maximum ray length: 0.7–2.9µm, avg. = 1.5µm, n = 105

Central depression width/central area width: 45.8–76.7%, avg. = 60.9%, n = 105

Ray length/Central area width: 17.8–65.3%, avg. = 39.1%, n = 105

Ray angle from radial: 2–16.2°, avg. = 7°, n = 105

Occurrence: latest Cenomanian (CC10b) – late Turonian (CC12)

Remarks: E. moratus can be differentiated from ancestral species *E. floralis* and *E. octopetalus* by possessing fewer wall elements/rays (7 vs. 9 and 8, respectively). The relatively large size of the central depression and radial pattern of the rays can be used to differentiate *E. moratus* from *L. septenarius* in well to moderately preserved material when using the criteria of >50% central depression/central area and <15° ray angle. Poorly preserved specimens overgrow and may superficially resemble *L. septenarius*. Careful observation through high to low focus can help consistently separate these two species, as *Eprolithus* exhibit rays that project from the wall elements as a continuous ridge between the proximal and distal sides of the fossil.

GENUS Lithastrinus (Stradner 1962) Varol 1992
Type species: *Lithastrinus grillii* Stradner 1962

Lithastrinus septenarius (Forchheimer)
Plate 1, figure 8; Plate 3, figures 3–4; Plate 5, figures 1–6

Lithastrinus moratus (Stover) VAROL 1992 Pl. 1, Fig. 17–18; Pl. 6, Fig. 6
Lithastrinus septenarius FORCHHEIMER 1972 p. 53, Pl. 24, Fig. 1–4; Pl. 27, Fig. 2

Diagnosis: A *Lithastrinus* consisting of 7 wall elements inclined and twisted about a narrow central depression/diaphragm less than half the width of the central area. Rays protrude only from the proximal and distal ends of each cycle of wall elements and do not project radially from the center. Ray angles are frequently greater than 15° and average 21°.

Description: Seven wall elements are arranged in an inclined, twisted ring of two stacked cycles around a central depression. This inclination of the elements creates a twisting motion while moving from high to low focus on a light microscope. The cycles are connected in the middle of this central depression by a thin plate, or diaphragm, of 7 overlapping lath-shaped elements. The central depression is narrow, less than half the width of the central area measured between rays, and is no wider than the small diaphragm itself. The central area is relatively bright in polarized light due to the thickness and constriction of the wall elements around the diaphragm. Rays project only from the proximal and distal ends of each wall element. This gives the appearance of a rounded "collar" of wall elements when focusing on the diaphragm in a light microscope and when seen in side view in SEM. The rays project from the central area at an angle usually greater than 15° up to ~44°

Measurements:

Central area width: 2.7–5.9µm, avg = 3.8µm, n = 297

Maximum ray length: 0.9–4.4µm, avg. 2.3µm, n = 297

PLATE 3

Light photomicrographs of specimens at ×1250 magnification. Scale bar at bottom right is 10 micrometers. XPL = cross polarized light, GP = gypsum plate, PL = plane light, PC = phase contrast.

1 *E. moratus*, e. Turonian, Site 1257B, Core 23, Section 1W, 10–11cm; 1a: XPL, 1b: GP, 1c–e: high through low focus, PL.

2 *E. moratus*, e. Turonian, Site 1257B, Core 23, Section 1W, 10–11cm; 2a: XPL, 2b: GP, 2c–e: high through low focus, PC.

3 *L. septenarius*, m. Santonian, Kure Beach Corehole, NJ 1551, 1100.7'; 3a: XPL, 3b: GP, 3c–e: high through low focus, PC.

4 *L. septenarius*, m. Santonian, Kure Beach Corehole, NJ 1551, 1100.7'; 4a: XPL, 4b: GP, 4c–e: high through low focus, PC.

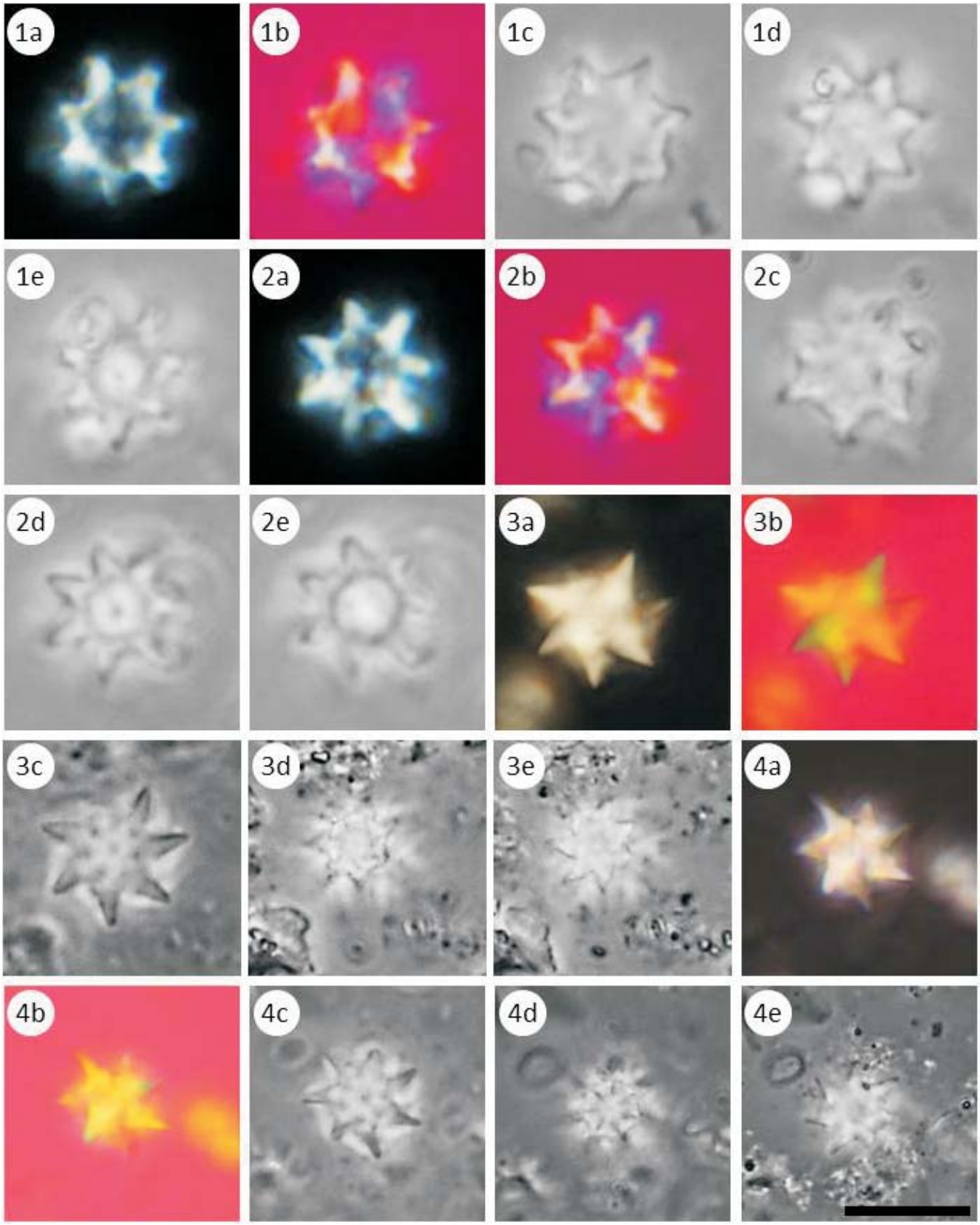
1a
1b
1c
1d
1e
2a
2b
2c
2d
2e
3a
3b
3c
3d
3e
4a
4b
4c
4d
4e

Central depression width/central area width: 19.2–60%, avg. = 38.8%, n = 297

Ray length/Central area width: 26.5–105.4%, avg. = 60.6%, n = 297

Ray angle from radial: 3.6–43.6°, avg. = 20.7°, n = 297

Occurrence: late Turonian (CC13)-middle Santonian (CC16)

Remarks: Lithastrinus septenarius is differentiated from *L. grilli* by having 7 as opposed to 6 wall elements. The relatively small size of the central depression and non-radial arrangement of the rays is used to separate *L. septenarius* from *E. moratus* in well to moderately preserved material. In poor samples *L. septenarius* retains the rounded appearance of the wall elements which form a "collar" around the diaphragm, a unique characteristic of *Lithastrinus*, whereas in *Eprolithus* the rays project continuously between the relative proximal and distal sides.

CONCLUSIONS

Detailed morphological analysis of 7-rayed *Eprolithus* and *Lithastrinus* morphotypes reveals important characteristics for the recognition of two different species in uppermost Cenomanian through lower Santonian sediments. Current taxonomic definitions of Turonian and Coniacian species *Eprolithus moratus* and *Lithastrinus septenarius* have been revised based on a number of new criteria to separate them both morphologically and stratigraphically while *Eprolithus eptapetalus* should be considered an invalid name. Splitting these species into separate genera is consistent with previous descriptions using the size of the opening in the central area and evidence of twisting in the surrounding wall elements. The 7-rayed *Eprolithus moratus* is distinguished from *Lithastrinus septenarius* by having a significantly larger central depression (i.e., a D/C = 0.5; text-figs. 3–4). It is evident from SEM photomicrographs that the actual elements of the diaphragm are already reduced in *E. moratus* as they are in *L. septenarius*, while the concave central depression surrounding them remains larger. In addition, it is crucial that special attention be paid to the nature of the rays as one focuses through a specimen. The rays should only project from the proximal and distal ends of the wall elements in *Lithastrinus*. This is particularly helpful with poorly preserved material where rays and central areas overgrow or dissolve. Ray angle from radial is also typically less than 15° in *E. moratus* (though there are some *Lithastrinus* with fairly straight rays as well) and ray length not much more than half the width (average of 53.3%) of the total central area. Outliers are likely specimens altered by diagenesis.

The descriptions of *L. septenarius* and *L. moratus*, as defined in this paper, provide more robust criteria for reproducing a reliable biostratigraphic datum. The ranges of *E. moratus* and *L. septenarius* are inconsistent with those predicted using the CC zonation and suggests zone CC13 and CC16 as originally defined may require revisions. Although they are rare, the last occurrence of *E. moratus* and first occurrence of *L. septenarius* in the uppermost Turonian are more consistent than zonal markers *Marthasterites* and *Liliasterites* and provide a very useful datum for the uppermost Turonian.

ACKNOWLEDGMENTS

We would like to acknowledge Jean Self-Trail and Jim Bergen for their taxonomic discussions and for loaning material for this study from the Kure Beach core and Stover's (1966) topotype material, respectively. Additional thanks to Mark Leckie for providing samples collected from the type section of the Mancos Shale at Mesa Verde and Bobbi Brace, Zachary Kita, and Jim Pospichal for their helpful critique. Special thanks to Harry Dowsett for his helpful review and recommended revisions. A special acknowledgement also to the funding sources of this research: the AAPG Rodney A. Bernasek Memorial Grant, GCSSEPM Ed Picou Fellowship Grant, and the University of Nebraska-Lincoln.

REFERENCES

BLACK, M., 1973. British Lower Cretaceous coccoliths. I. Gault Clay. *Paleontological Society Monographs*, 1: 1–48.

BRALOWER, T. J. and BERGEN, J. A., 1998. Cenomanian–Santonian calcareous nannofossil biostratigraphy of a transect of cores drilled across the Western Interior Seaway. In: Dean, W. E. and Arthur, M. A., Eds. *Stratigraphy and paleoenvironments of the Cretaceous Western Interior Seaway, USA,* 59–77. Tulsa, OK: Society for Sedimentary Geology (SEPM). Concepts in Sedimentology and Paleontology, 6.

BURNETT, J. A. (with contributions from GALLAGHER, L. T. and HAMPTON, M. J.), 1998. Upper Cretaceous. In: Bown, P. R., Ed.. *Calcareous nannofossil biostratigraphy,* 132–199*,* London: Chapman and Hall/Kluwer Academic Publishers. British Micropalaeontological Society Publications Series.

PLATE 4

SEM Photomicrographs of *E. moratus*, e. Turonian, Site 1257B, Core 23, Section 1W, 10–11cm.
Scale bars are 1 micrometer. 1–6, ×10,000.

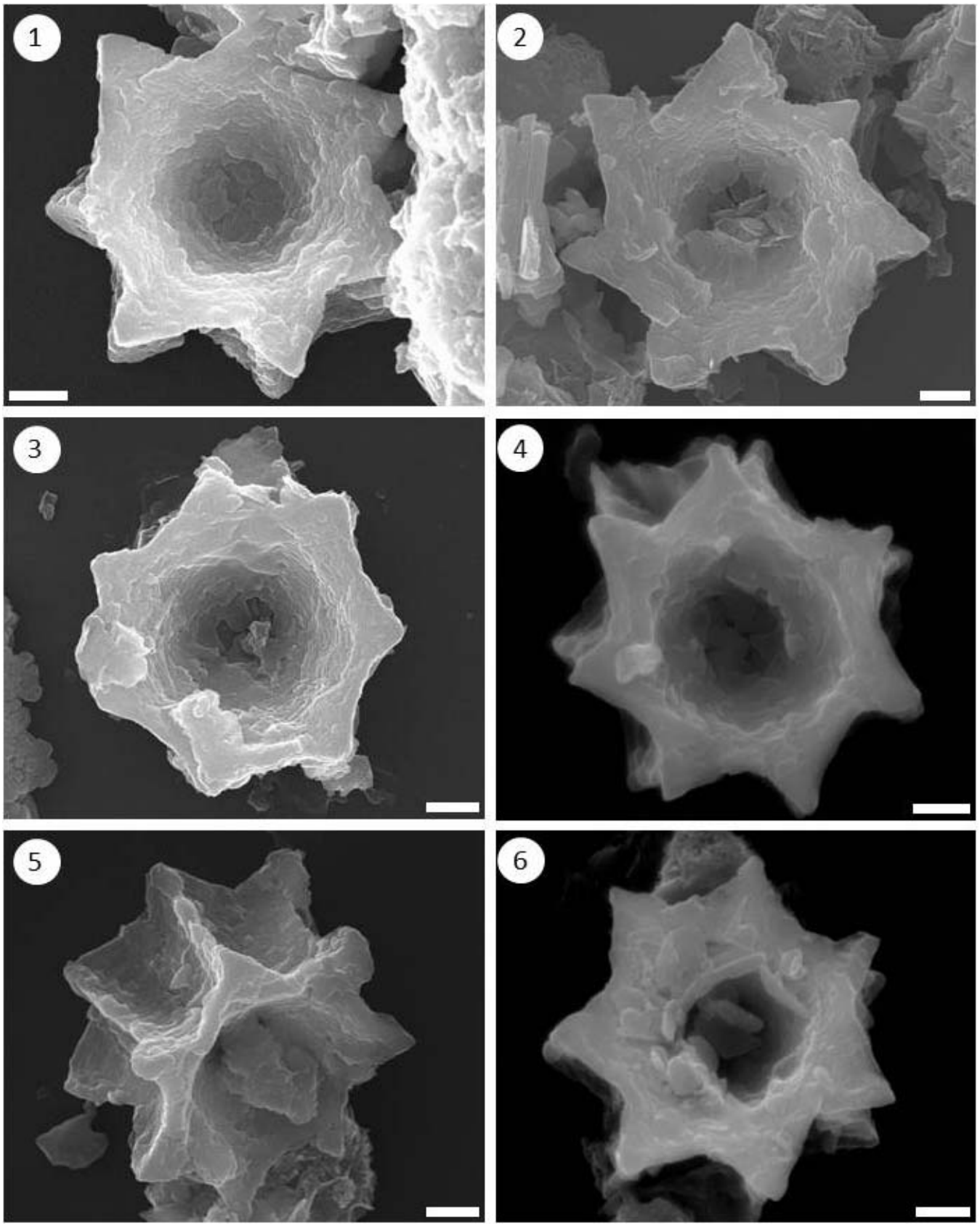
1
2
3
4
5
6

DEFLANDRE, G., 1959. Sur les nannofossiles calcaires et leur systématique. *Revue de Micropaléontologie*, 2: 127–152.

DEFLANDRE, G. and FERT, C., 1954. Observations sur les Coccolithophoridés actuels et fossils en microscopie ordinaire et électronique. *Annales de Paléontologie*, 40: 115–176.

FORCHHEIMER, S., 1972. Scanning electron microscope studies of Cretaceous coccoliths from the Köpingsberg Borehole No. 1, SE Sweden. *Sveriges Geologiska Undersökning*, ser. C, 668, 65: 14: 1–141.

GEISEN, M., BOLLMAN, J., HERRLE, J. O., MUTTERLOSE, J. and YOUNG, J. R., 1999. Calibration of the random settling technique for calculation of absolute abundances of calcareous nannoplankton. *Micropaleontology.* 45: 437–442.

GRADSTEIN, F. M., OGG, J. G., SMITH, A. G., et al., 2004. *A Geologic Time Scale 2004*. Cambridge: Cambridge University Press,500 pp.

HAMMER, Ø. and HARPER, D., 2006. *Paleontological data analysis*. Malden, MA: Blackwell Publishing. 351 pp.

HARDAS, P. and MUTTERLOSE, J., 2006. Calcareous nannofossil biostratigraphy of the Cenomanian/Turonian boundary interval of ODP Leg 207 at the Demerara Rise. *Revue de Micropaléontologie*, 49: 165–179.

LEES, J. A., 2002. Calcareous nannofossil biogeography illustrates paleoclimatic change in the Late Cretaceous Indian Ocean. *Cretaceous Research*, 23: 537–634.

———, 2008. The Calcareous nannofossil record across the Late Cretaceous Turonian/Coniacian boundary, including new data from Germany, Poland, the Czech Republic and England. *Cretaceous Research*, 29: 40–64.

LECKIE, R. M., KIRKLAND, J. I. and ELDER, W. P., 1997. Stratigraphic framework and correlation of a principal reference section of the Mancos Shale (Upper Cretaceous), Mesa Verde, CO. In: Anderson, O. J., Kues, B. C., and Lucas, S. G., Eds., *Mesozoic geology and paleontology of the Four–Corners Region, 48th Guidebook,* 163–216: Albuquerque: New Mexico Geological Society.

LECKIE, R. M., YURETICH, R. F., WEST, O. L. O., FINKELSTEIN, D. and SCHMIDT, M., 1998. Paleoceanography of the southwestern Western Interior Sea during the time of the Cenomanian–Turonian boundary (Late Cretaceous). In: Dean, W. E. and Arthur, M. A., Eds. *Stratigraphy and paleoenvironments of the Cretaceous Western Interior Seaway, USA,* 101–126. Tulsa, OK: Society for Sedimentary Geology (SEPM). Concepts in Sedimentology and Paleontology, 6.

LINNERT, C., MUTTERLOSE, J. and ERBACHER, J., 2010. Calcareous nannofossils of the Cenomanian/Turonian boundary interval from the boreal realm (Wunstorf, northwest Germany). *Marine Micropaleontology*, 74: 38–58.

MANIVIT, H., PERCH-NIELSEN, K., PRINS, B. and VERBEEK, J. W., 1977. Mid-Cretaceous calcareous nannofossils biostratigraphy. *Proceedings of the Koninklijke Nederlandse Akademie van Wetenschappen*, 80: 169–181.

OCEAN DRILLING STRATIGRAPHIC NETWORK (ODSN), 2011. *Plate tectonic reconstruction service*, http: //www.odsn.de/odsn/services/paleomap/paleomap.html.

OGG, J. and LUGOWSKI, A., 2012. *TS Creator visualization of enhanced Geologic Time Scale 2004 database (Ver. 5.0; 2012*), http: //www.tscreator. org.

PERCH-NIELSEN, K., 1968. Der Feinbau und die Klassifikation der Coccolithen aus dem Maastrichtien von Dänemark. *Det kongelige Danske Videnskabernes Selskab Biologiske Skrifter*, 16: 1–93.

———,1979. Calcareous nannofossils from the Cretaceous between the North Sea and the Mediterranean. *IUGS Series A*, 6: 223–272.

———,1985. Mesozoic calcareous nannofossils. In: Bolli, H. M., Saunders, J. B. and Perch-Nielsen, K., Eds., *Plankton stratigraphy*, 1: 329–426.

RASBAND, W. S., 1997–2012. *ImageJ.* Bethesda, MD: U. S. National Institutes of Health, http: //imagej.nih.gov/ij/.

SISSINGH, W., 1977. Biostratigraphy of Cretaceous calcareous nannoplankton. *Geologie en Mijnbouw*, 56: 37–65.

SHAMROCK, J. L. and WATKINS, D. K., 2009. Evolution of the Cretaceous calcareous nannofossil genus *Eiffellithus* and its biostratigraphic significance. *Cretaceous Research*, 30: 1083–1102.

STOVER, L. E., 1966. Cretaceous coccoliths and associated nannofossils from France and the Netherlands. *Micropaleontology*, 12: 133–167.

STRADNER, H., 1962. Über neue und wenig bekannte Nannofossilien aus Kreide und Alttertiär. *Sonderdruck Verhandlungen der Geologischen Bundesanstalt (Wein)*, 2: 363–377.

STRADNER, H. and STEINMETZ, J., 1984. Cretaceous calcareous nannofossils from the Angola Basin, Deep Sea Drilling Project Site 530. In: Amidei, R., et al., *Initial Reports of the Deep Sea Drilling Project*, *75*, 565–649. Washington, DC: U. S. Government Printing Office.

PLATE 5

SEM Photomicrographs of *L. septenarius*, m. Santonian, Kure Beach Corehole, 1100.7 ft. Scale bars are 1 micrometer.

1 ×15,000

2 ×10,000

3 ×10,000

4 ×8,000

5 side view; ×10,000

6 side view; ×9,000.

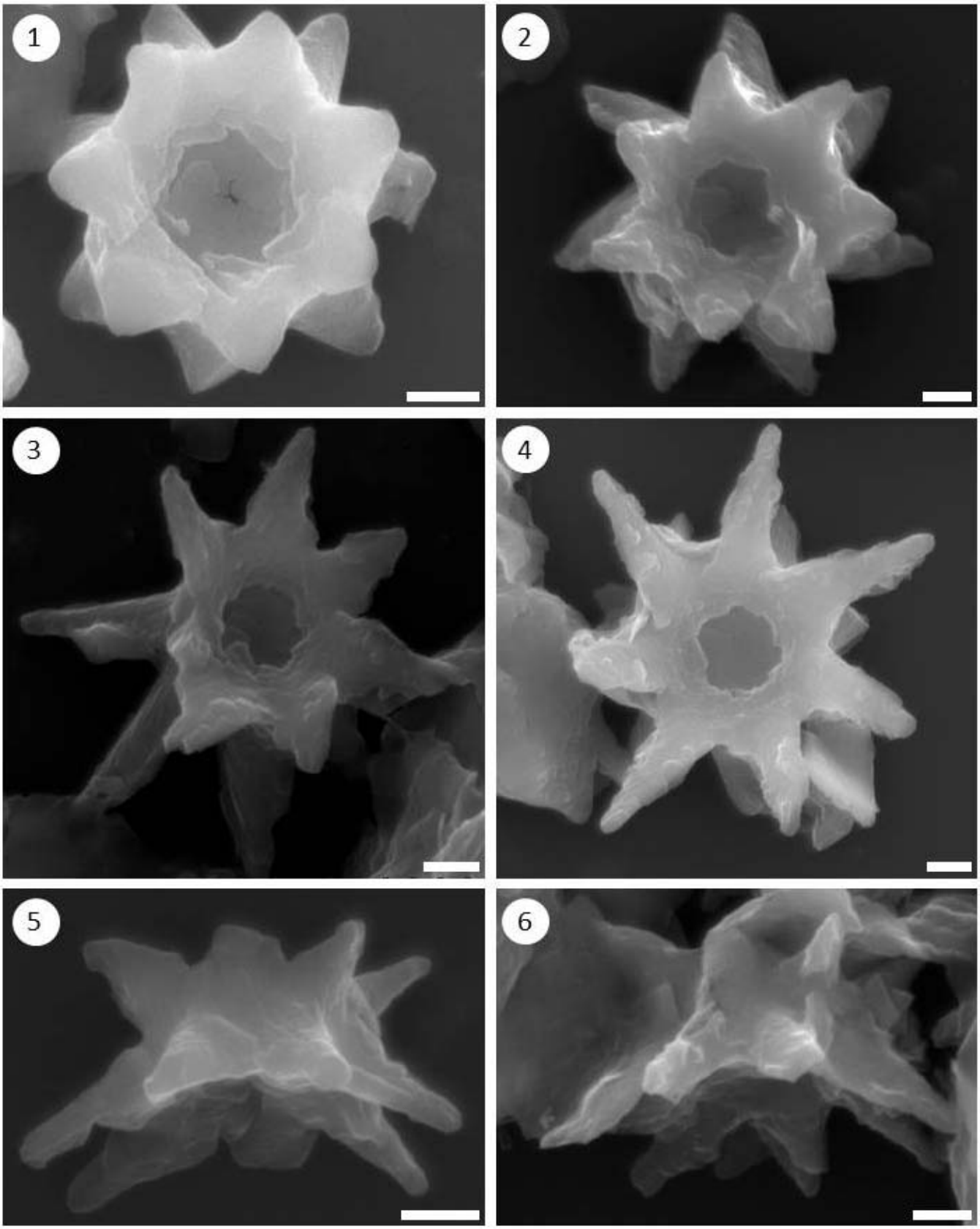
1
2
3
4
5
6

THIERSTEIN, H. R., 1973. Lower Cretaceous calcareous nannoplankton biostratigraphy. *Abhandlungen der Geologischen Bundesanstalt (Wein),* 29: 1–52.

VAROL, O., 1992. Taxonomic revision of the Polycyclolithaceae and its contribution to Cretaceous biostratigraphy. *Newsletters on Stratigraphy*, 27: 93–127.

VEKSHINA, V. N., 1959. Coccolithophoridae of the Maastrichtian deposits of the West Siberian lowlands. *Siberian Science Research Institute of Geology, Geophysics, Mineralogy, and Raw Materials*, 2: 56–81

WATKINS, D. K., 1985. Biostratigraphy and paleoecology of calcareous nannofossils in the Greenhorn marine cycle. In: Pratt, L. M., Kauffman, E. G. and Zelt, F. B., Eds., *Fine-grained deposits and biofacies of the Cretaceous Western Interior Seaway: Evidence of cyclic sedimentary processes,* 151–156. Tulsa, OK: Society of Economic Paleontologists and Mineralogists. SEPM Field Trip Guidebook No. 4.

WATKINS, D. K. and BERGEN, J. A., 2003. Late Albian adaptive radiation in the calcareous nannofossil genus *Eiffellithus*. *Micropaleontology*, 49: 231–252.

WATKINS, D. K., SHAFIK, S. and SHIN, I. C., 1998. Calcareous nannofossils from the Cretaceous of the Deep Ivorian Basin. In: Mascle, J., Lohman, G. P. and Moullade, M., et al., *Proceedings of the Ocean Drilling Program, Scientific Results 159,* 319–333. College Station, TX: Ocean Drilling Program.

WEST, O. L. O., LECKIE, R. M. and SCHMIDT, M., 1998. Foraminiferal paleoecology and paleoceanography of the Greenhorn cycle along the southwestern margin of the Western Interior Sea. In: In: Dean, W. E. and Arthur, M. A., Eds., *Stratigraphy and paleoenvironments of the Cretaceous Western Interior Seaway, USA,* 79–99. Tulsa, OK: Society for Sedimentary Geology (SEPM). Concepts in Sedimentology and Paleontology, 6.

Received
Accepted
Published August 2014

PLATE 6

Light photomicrographs of *E. moratus* at 1250x magnification. Scale bar at bottom right is 10 micrometers. XPL = cross polarized light, PL = plane light, PC = phase contrast.

1 *E. moratus*, e. Turonian, Site 959D, Core 68R, Section 1, 14–15cm; 1a: XPL, 1b: PC.

2 *E. moratus*, e. Turonian, Site 1257B, Core 23, Section 1W, 10–11cm; 2a: XPL, 2b: PC.

3 *E. moratus*, e. Turonian, Site 1257B, Core 23, Section 1W, 10–11cm; 3a: XPL, 3b: PC.

4 *E. moratus*, e. Turonian, Site 1257B, Core 23, Section 1W, 10–11cm; 4a: XPL, 4b: PC.

5 *E. moratus*, m.-l. Turonian, northern France, Stover (1966), sample 9 (type sample for *E. moratus*); 5a: XPL, 5b–d: high through low focus, PL.

6 *E. moratus*, e. Turonian, northern France, Stover (1966), sample 13; 6a: XPL, 6b–d: high through low focus, PL.

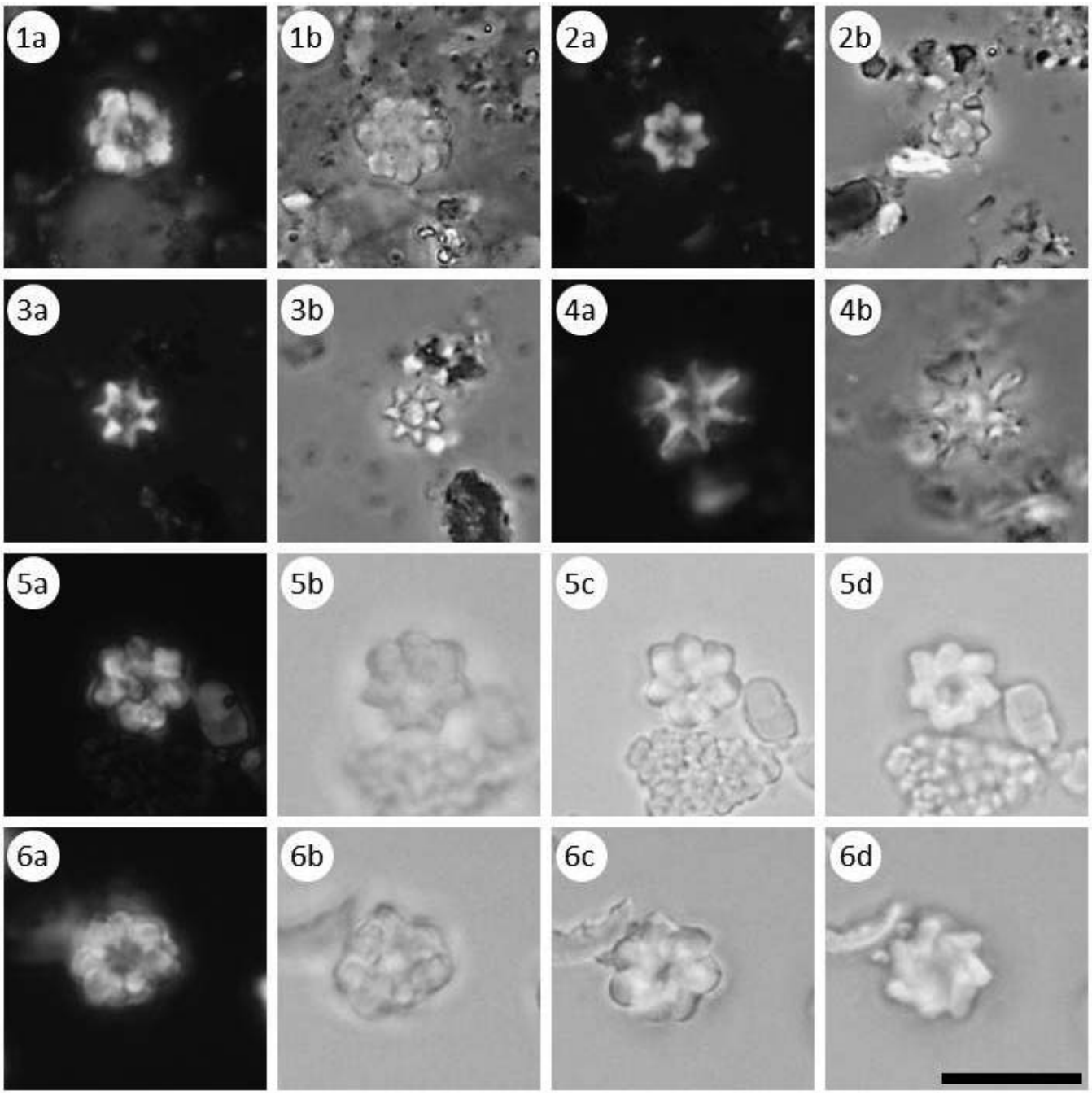
1a
1b
2a
2b
3a
3b
4a
4b
5a
5b
5c
5d
6a
6b
6c
6d